Angle-resolved spectroscopy study of Ni-based superconductor $SrNi_2As_2$

L.-K. Zeng,[1] P. Richard,[1,2,*] A. van Roekeghem,[1,3] J.-X. Yin,[1] S.-F. Wu,[1] Z. G. Chen,[1] N. L. Wang,[4,2] S. Biermann,[3,5,6] T. Qian,[1,2,†] and H. Ding[1,2,‡]

[1]*Beijing National Laboratory for Condensed Matter Physics and Institute of Physics, Chinese Academy of Sciences, Beijing 100190, China*

[2]*Collaborative Innovation Center of Quantum Matter, Beijing, China*

[3]*Centre de Physique Théorique, Ecole Polytechnique, CNRS-UMR 7644, Université Paris-Saclay, 91128 Palaiseau, France*

[4]*International Center for Quantum Materials, School of Physics, Peking University, Beijing 100871, China*

[5]*Collège de France, 11 place Marcelin Berthelot, 75005 Paris, France*

[6]*European Theoretical Synchrotron Facility, Europe*

(Received 15 April 2016; revised manuscript received 15 July 2016; published 29 July 2016)

We performed an angle-resolved photoemission spectroscopy study of the Ni-based superconductor $SrNi_2As_2$. Electron and hole Fermi surface pockets are observed, but their different shapes and sizes lead to very poor nesting conditions. The experimental electronic band structure of $SrNi_2As_2$ is in good agreement with first-principles calculations after a slight renormalization (by a factor 1.1), confirming the picture of Hund's exchange-dominated electronic correlations decreasing with increasing filling of the 3*d* shell in the Fe-, Co-, and Ni-based compounds. These findings emphasize the importance of Hund's coupling and 3*d*-orbital filling as key tuning parameters of electronic correlations in transition-metal pnictides.

DOI: 10.1103/PhysRevB.94.024524

I. INTRODUCTION

Although isostructural counterparts of the Fe-based superconductors La(O,F)FeAs [1] and $(Ba,K)Fe_2As_2$ [2] can be synthesized using 3*d* transition-metal atoms other than Fe, superconductivity is found only in Ni-based LaONi*Pn* [3,4] and ANi_2Pn_2 [5–7] (A = Ca, Sr, and Ba, Pn = P and As), albeit with much lower superconducting transition temperature (T_c) values than in the Fe-based superconductors. Unlike the Fe-based family of superconductors, the parent compounds of the Ni-based superconductors do not show any magnetic ordering. While electronic correlations are responsible for a renormalization of the band structure of the Fe-based superconductors by a typical factor of 2–5 [8,9], recent angle-resolved photoemission spectroscopy (ARPES) study reported that the band dispersions are renormalized by a factor of 1–2 in $BaNi_2P_2$ [10] and by a factor of 1.4 in $TlNi_2Se_2$ [11], suggesting weaker electronic correlations in the Ni-based superconductors. Since Hund's coupling is believed to play a significant role to tune the correlation strength in these materials, a systematic study and comparison is of importance. Investigating the details of the electronic structure of the 122-Ni*Pn* materials thus appears a good starting point for understanding the key parameters for Fe-based superconductivity. Among the Ni-based superconductors, $SrNi_2As_2$ is particularly interesting. Superconductivity in this material is found at $T_c = 0.62$ K, and unlike $BaNi_2As_2$ and $SrNi_2P_2$, $SrNi_2As_2$ share the same tetragonal crystal structure as $(Ba,K)Fe_2As_2$ at high temperature, and no structural transition was reported in $SrNi_2As_2$ upon cooling.

In this paper, we present ARPES results on the Ni-based superconductor $SrNi_2As_2$. We observe small electronic correlations as compared with the Fe-based superconductors, without detectable orbital selectivity. We show that although the Hund's coupling tunes the correlations in the Fe compounds, its effect is limited in the Co and Ni compounds due to the large 3*d* shell electron filling. Therefore, in 3*d* compounds both Hund's coupling and shell electron filling play important roles in explaining the electronic correlations. The absence of magnetic order in $SrNi_2As_2$ is probably associated with the poor Fermi surface nesting conditions derived from the measured Fermi surfaces, as well as the negligible local moment due to the weakness of the electronic correlations.

II. EXPERIMENT

High-quality single crystals of $SrNi_2As_2$ were grown by the flux method. ARPES experiments were performed at beamline PGM of the Synchrotron Radiation Center (Wisconsin) equipped with a Scienta R4000 analyzer. The energy and angular resolutions were set at 15–30 meV and 0.2°, respectively. The samples were cleaved *in situ* and measured in a vacuum better than 5×10^{-11} Torr. The Fermi level (E_F) of the samples was referenced to that of a gold film evaporated onto the sample holder. The high-symmetry points associated to the first Brillouin zone (BZ) of $SrNi_2As_2$ are defined in Fig. 1(a), along with their two-dimensional (2D) projections. Following our previous notations, the various cuts are indexed using the 1 Ni/unit cell, with the parameter a corresponding to the distance between two Ni atoms.

III. RESULTS AND DISCUSSION

The Fermi surface (FS) mappings of $Sr_2Ni_2As_2$ obtained by integrating the ARPES intensity within ±5 meV of E_F in the $k_z \sim 0$ and $k_z \sim \pi$ planes are displayed in Figs. 1(c) and 1(d), respectively. The Fermi wave vector (k_F) positions extracted from the band dispersions are also plotted. The results are quite different from those obtained for the Fe-based superconductors

*p.richard@iphy.ac.cn
†tqian@iphy.ac.cn
‡dingh@iphy.ac.cn

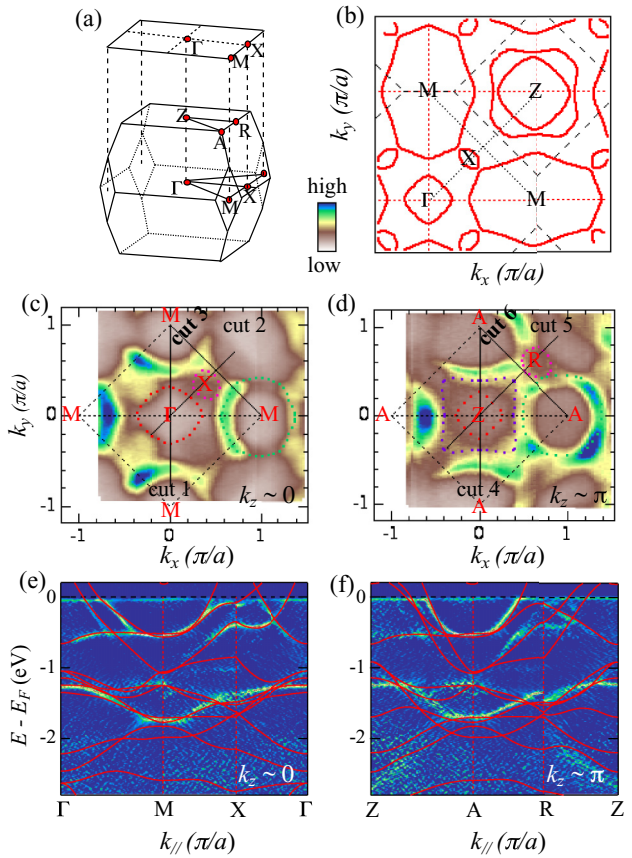

FIG. 1. (a) 3D BZ and projection in the 2D BZ, along with the definitions of high-symmetry points. (b) Calculated LDA FS. (c) and (d) ARPES mapping intensity plots at E_F recorded at 30 K on $SrNi_2As_2$ in the $k_z \sim 0$ and $k_z \sim \pi$ planes, respectively. The intensity is obtained by integrating the spectra within ± 5 meV with respect to E_F. The k_F positions are indicated by dots. (e) and (f) 2D curvature intensity plot along high-symmetry lines recorded at 30 K in the $k_z \sim 0$ and $k_z \sim \pi$ planes, respectively. The LDA band structure renormalized by a factor 1.1 is overlapped for comparison.

[8]. At $k_z \sim 0$, a rather squarish, relatively small hole pocket is detected at the Γ point, and a large electron pocket with an approximately hexagonal shape is observed at the M point. In addition, a small hole pocket is found slightly away from the X point. This FS topology is very similar to that measured in the $k_z \sim \pi$ plane, except that an additional hole pocket is found at Z for $k_z \sim \pi$, suggesting that one band has a strong three-dimensional (3D) character, while the other FSs are more quasi-2D. We also note that the sizes and shapes of the Γ-centered hole pockets differ significantly from those of the M-centered electron pocket, which means that the electron-hole quasinesting is poor in this system. Qualitatively, the experimental data are quite consistent with the local density approximation (LDA) calculations presented in Fig. 1(b).

Figures 1(e) and 1(f) show the 2.8-eV-wide 2D curvature [12] intensity plots along the Γ-M-X-Γ momentum path at $k_z \sim 0$ and the Z-A-R-Z momentum path at $k_z \sim \pi$, respectively. For comparison, we superimpose the LDA bands on top of the experimental data. The experimental band dispersions show excellent agreement with the LDA calculations after an overall renormalization by a factor of 1.1.

For a closer look at the low-energy states, we present in Fig. 2 ARPES intensity cuts along some high-symmetry lines, along with the corresponding intensity plots of curvature and either the related energy dispersion curve (EDC) or momentum distribution curve (MDC) plots. In particular, the top row shows clearly that while only two bands (labeled as α and β) cross E_F along Γ-M ($k_z = 0$), a third band (γ) emerges at E_F along Z-A ($k_z = \pi$), which is consistent with our FS mappings. The η and δ bands together form a hole pocket around the X point.

As compared with the Fe-based superconductors, the LDA calculations match the experimental results very well and the band renormalization is very small for $SrNi_2As_2$. The small renormalization factor (1.1) indicates that the electronic correlations in $SrNi_2As_2$ are much weaker than that in the Fe-based superconductors, in which the overall bandwidth is typically renormalized by a factor of 2–5 [8,9]. In addition, we do not observe in $SrNi_2As_2$ any indication of orbital selectivity, which contrasts with the Fe-pnictide superconductors, for which the bands with d_{xy} character are renormalized twice as much as the other bands [13]. The weak electronic correlations in $SrNi_2As_2$ go hand in hand with small local moments and absence of magnetic ordering. In an itinerant picture, the absence of good FS nesting conditions prevents the formation of a spin-density wave.

In Fig. 3 we compare the renormalization factor of different transition-metal pnictides with the 122 structure. A clear monotonic but nonlinear decrease in the overall renormalization factor is observed as the filling of the $3d$ shell increases from $3d^6$ in $BaFe_2As_2$ [14] to $3d^{10}$ in $BaCu_2As_2$ [15]. This is consistent with the scenario that the electronic correlations are tuned by the electron filling of the $3d$ shell [16]. Although the Hund's coupling is vital in Fe compounds, we find in our calculations that its role for the electronic correlations is limited in the Co and Ni compounds. The sudden drop of electronic correlation strength from Fe compounds to Co compounds followed by a much smaller slope is mainly due to $3d$ electron filling.

To address the effect of the Hund's coupling and the influence of the filling of the Ni-$3d$ shell in $SrNi_2As_2$, we have performed dynamical mean-field theory (DMFT) calculations of the self-energy (for a review, see [17]) at different physical and artificial fillings. The effective Hubbard interactions have been calculated within the constrained random phase approximation [18] in the implementation of Ref. [19]. The construction of the Hamiltonian corresponds to what is commonly called a "d-dp Hamiltonian" in the literature [20,21], that is, Ni d- and As p-derived bands are included in the noninteracting part of the Hamiltonian, and Hubbard interactions are added for the Ni d states. The values obtained for the Slater integrals are $F_0 = 3.55$ eV, $F_2 = 8.08$ eV, and $F_4 = 5.78$ eV. This corresponds to a Hubbard energy $U = 3.55$ eV and a Hund's coupling $J = 0.99$ eV, which is notably stronger than in $BaFe_2As_2$ or $BaCo_2As_2$ [13,22]. Double counting of correlations is avoided using the correction of the "around-mean-field" form [23].

We perform calculations for $SrNi_2As_2$ and for artificial compounds where we removed one and two electrons with respect to the filling of the physical $SrNi_2As_2$ compound. This is done by determining the chemical potential corresponding

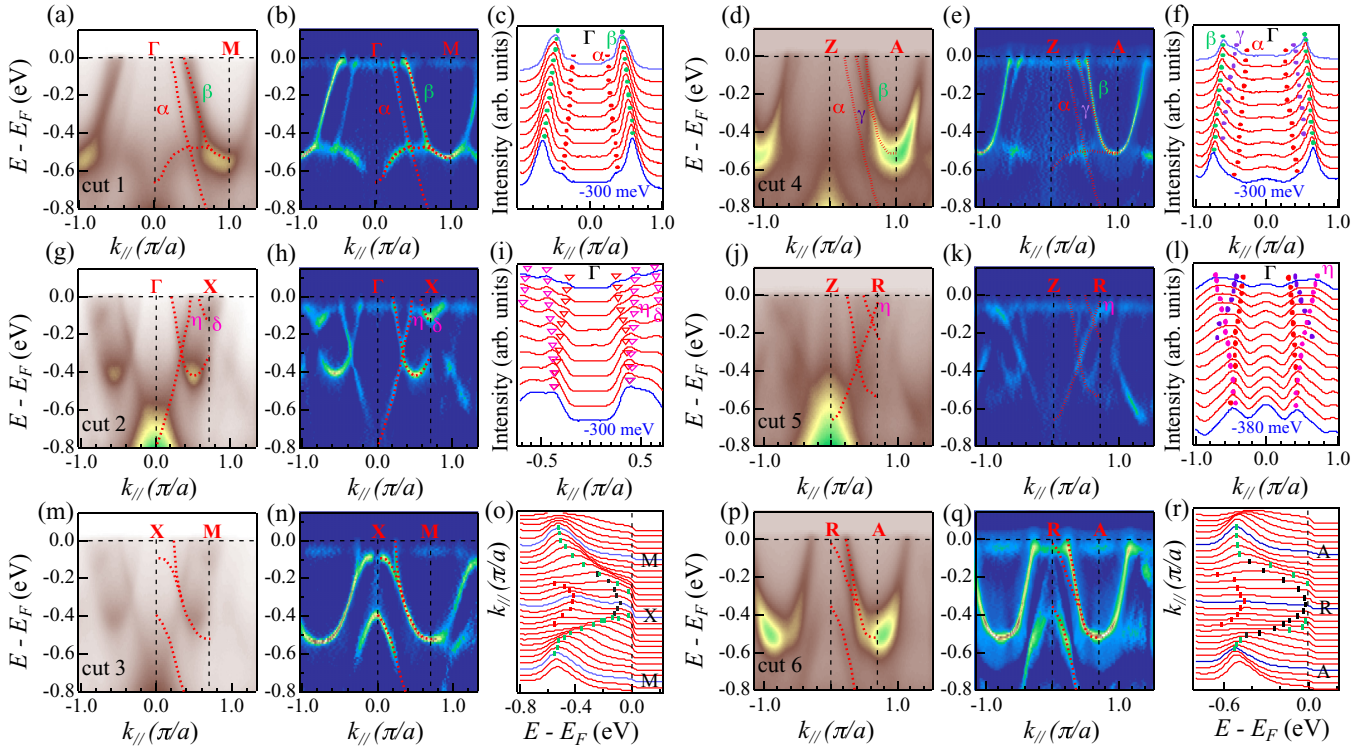

FIG. 2. ARPES data recorded on $SrNi_2As_2$ along different high-symmetry lines [the cuts correspond to those in Figs. 1(c) and (d)]. The three left columns refer to $k_z = 0$, while the three right columns correspond to $k_z = \pi$. The first [(a), (g), (m)] and fourth [(d), (j), (p)] columns correspond to ARPES intensity plots. The second [(b), (h), (n)] and fifth [(e), (k), (q)] columns correspond to the intensity of 2D curvature of the corresponding ARPES intensity plots. The third and sixth columns are associated to either MDC [(c), (i), (f), (l)] plots or EDC [(o), (r)] plots of the corresponding ARPES intensity plots. The peak positions are identified with symbols.

to these respective electron counts. In Fig. 4, we show the imaginary part of the self-energy Σ as a function of (imaginary) Matsubara frequencies for all three situations. We also compare this result with analogous calculations in which we put the Hund's coupling to zero (i.e., $F_2 = F_4 = 0$ in terms of the Slater integrals). In a Fermi liquid, the imaginary part of Σ on the Matsubara axis vanishes linearly, and the slope is related to the quasiparticle residue Z as

$$Z = \frac{1}{1 - \frac{\partial \Sigma(i\omega)}{\partial i\omega}}. \quad (1)$$

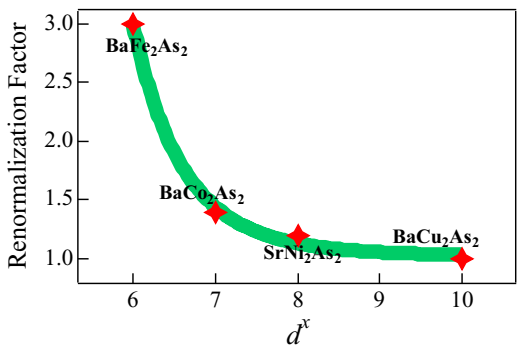

FIG. 3. Relationship between the renormalization factor and the number of 3*d* electrons for Fe- [14], Co- [13], Ni- and Cu-based [15] 122-structure materials.

Within DMFT, Σ is purely local and Z directly equals the inverse effective mass enhancement. For $SrNi_2As_2$, we obtain

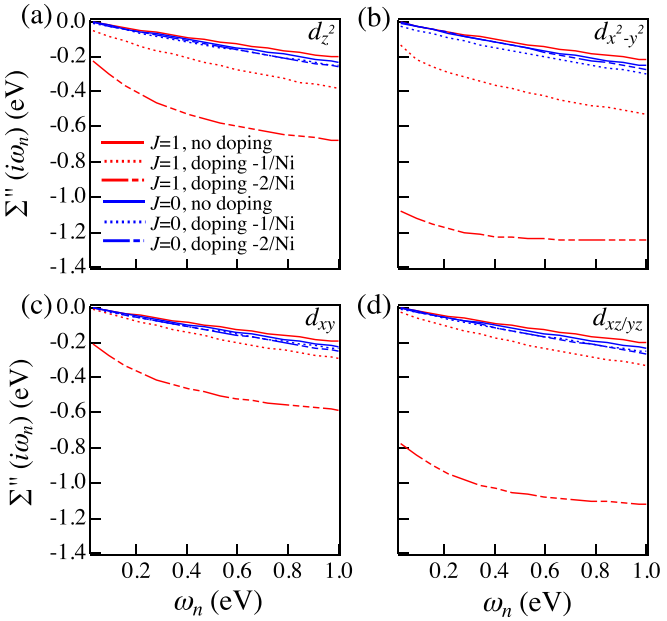

FIG. 4. Imaginary part of the self-energy for orbitals (a) d_{z^2}, (b) $d_{x^2-y^2}$, (c) d_{xy}, (d) $d_{xz/yz}$ as a function of the Matsubara frequency for $SrNi_2As_2$ and hypothetical compound consisting of $SrNi_2As_2$ with one and two electrons removed with respect to the filling of the physical $SrNi_2As_2$ compound.

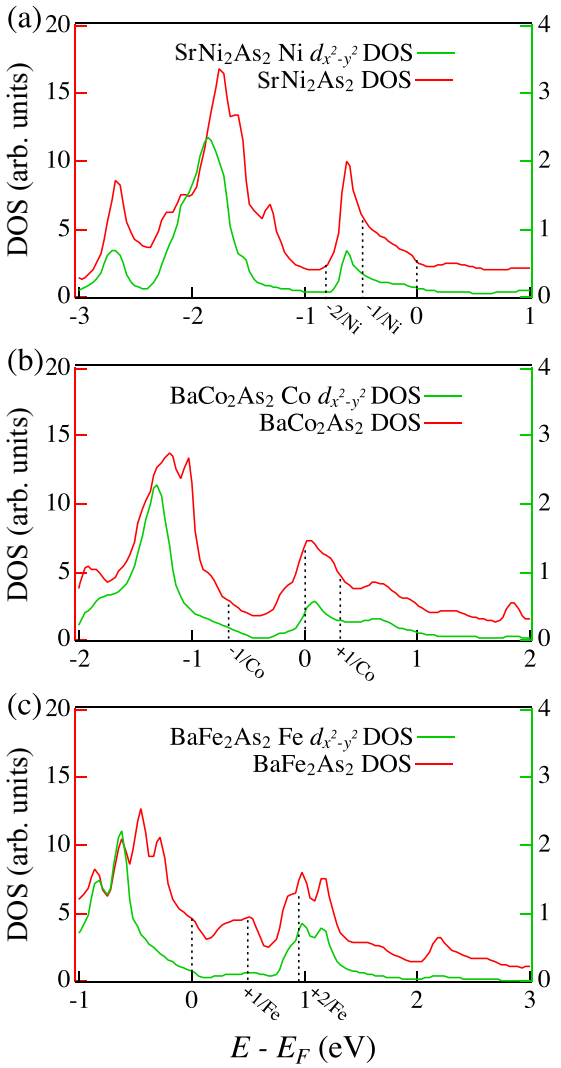

FIG. 5. Total and $d_{x^2-y^2}$ density of states for (a) $SrNi_2As_2$, (b) $BaCo_2As_2$, and (c) $BaFe_2As_2$. The dashed lines correspond to doping levels 0, −1, −2 electron(s) per Ni for $SrNi_2As_2$; +1, 0, −1 electron(s) per Co for $BaCo_2As_2$; and +2, +1, 0 electron(s) per Fe for $BaFe_2As_2$, respectively.

an effective mass of $m^*/m = 1.2$–1.3 in good agreement with the experiment. The orbital dependence of the effective mass enhancement is negligible in this case. Interestingly, the effect of the electronic correlations is found to be even weaker than in the case of vanishing Hund's coupling $J = 0$, in contrast to what was found in $BaFe_2As_2$ or $BaCo_2As_2$ [13,22,24]. Such a behavior is consistent with the scenario of the influence of Hund's coupling developed in the literature [24–27]. The key parameter is the large filling of the Ni-3d shell. Indeed, the constructed Wannier orbitals contain 8.8 electrons due to the Ni-As hybridization that increases the number of electrons in the Ni-3d shell with respect to the nominal electron count of eight electrons per Ni. When this number of electrons is reduced by one per Ni atom, the effect of correlations is slightly enhanced by the Hund's coupling and a small orbital dependency is retrieved.

In Fig. 5 we note, in particular, the more strongly correlated behavior of the $d_{x^2-y^2}$-derived band, which has a large density close to E_F. This effect becomes huge when two electrons per Ni atom are removed. It is even more pronounced than in $BaFe_2As_2$ due to the larger value of the Hund's coupling. Interestingly, the most correlated orbital in this case is still $d_{x^2-y^2}$, in contrast to $BaFe_2As_2$ where at this filling the d_{xy} orbital is the most strongly correlated. We have traced back this difference to a more pronounced 3D character in $SrNi_2As_2$ caused by the reduction of the c/a ratio with respect to those of $BaFe_2As_2$ and $BaCo_2As_2$. Indeed, the larger dispersion of out-of-plane bands, in particular in the $k_z = \pi$ plane, leaves the flat $d_{x^2-y^2}$ band at E_F when two electrons per Ni are removed in the Ni compound [the band around $E_B = -0.808$ eV in Fig. 1(f)], while the density of states of this orbital presents a pseudogap near E_F in the Fe compound [28], i.e., a strong suppression of density of states, as shown by the green curve in Fig. 5(c). The presence of the flat band at E_F is strongly reminiscent of the case of undoped $BaCo_2As_2$ [13,29]. In the latter compound, the physics is very strongly dependent on the precise energetic position of this flat band, which determines its paramagnetic behavior (in contrast to ferromagnetic $CaCo_2As_2$ [30]). Yet, the overall degree of correlations in $BaCo_2As_2$ is weak. This suggests the global filling to be the key tuning parameter for the correlation strength. The details of the density of states, including van Hove singularities close to E_F, then intervene to tune the orbital dependence of the correlations. Finally, we note again that the effect of correlations is weak and largely independent of the filling when no Hund's coupling is present. This demonstrates once more the importance of this quantity to tune the electronic correlations in transition-metal pnictides, from stronger (as in Fe pnictides) to weaker correlations (as in $SrNi_2As_2$).

IV. SUMMARY

In summary, we have studied the electronic structures of the Ni-based superconductors $SrNi_2As_2$. One additional hole Fermi surface around the BZ center Z point is observed compared to the Γ point, which indicates a strong three dimensionality. Our results are in good agreement with LDA calculations, albeit for a small overall, orbital insensitive renormalization factor of 1.1, suggesting that the electronic correlations in these compounds are weak compared to the Fe-based superconductors. The nonlinear reduction of the electronic correlation strength with the increasing filling of the 3d shell for the Fe-, Co- and Ni-based compounds confirms that 3d electron filling plays an important role in tuning the electronic correlations, which may be related to higher T_c's in the Fe-based materials. Although we observe both hole and electron FS pockets separated by the same wave vector as in the Fe-based superconductors, the FS nesting is quite poor, which is possibly a reason for the absence of long-range magnetic order in $SrNi_2As_2$, along with the negligible local moments.

ACKNOWLEDGMENTS

We acknowledge X. X. Wu for useful discussions. This work was supported by grants from MOST (Grants No. 2011CBA001000, No. 2011CBA00102, No. 2012CB821403, No. 2013CB921703, and No. 2015CB921301) and NSFC

(Grants No. 11004232, No. 11034011/A0402, No. 11234014, and No. 11274362) from China, as well as by a Consolidator Grant (Project No. 617196) of the European Research Council.

[1] Y. Kamihara, T. Watanabe, M. Hirano, and H. Hosono, J. Am. Chem. Soc. **130**, 3296 (2008).
[2] Marianne Rotter, Marcus Tegel, and Dirk Johrendt, Phys. Rev. Lett. **101**, 107006 (2008).
[3] T. Watanabe, H. Yanagi, T. Kamiya, Y. Kamihara, H. Hiramatsu, M. Hirano, and H. Hosono, Inorg. Chem. **46**, 7719 (2007).
[4] Z. Li, G. Chen, J. Dong, G. Li, W. Hu, D. Wu, S. Su, P. Zheng, T. Xiang, N. Wang, and J. Luo, Phys. Rev. B **78**, 060504 (2008).
[5] Y. Tomioka, S. Ishida, M. Nakajima, T. Ito, H. Kito, A. Iyo, H. Eisaki, and S. Uchida, Phys. Rev. B **79**, 132506 (2009).
[6] F. Ronning, N. Kurita, E. D. Bauer, B. L. Scott, T. Park, T. Klimczuk, R. Movshovich, and J. D. Thompson, J. Phys.: Condens. Matter **20**, 342203 (2008).
[7] E. D. Bauer, F. Ronning, B. L. Scott, and J. D. Thompson, Phys. Rev. B **78**, 172504 (2008).
[8] P. Richard, T. Sato, K. Nakayama, T. Takahashi, and H. Ding, Rep. Prog. Phys. **74**, 124512 (2011).
[9] Ambroise van Roekeghem, Pierre Richard, Hong Ding, and Silke Biermann, C. R. Phys. **17**, 140 (2016).
[10] S. Ideta, T. Yoshida, M. Nakajima, W. Malaeb, H. Kito, H. Eisaki, A. Iyo, Y. Tomioka, T. Ito, K. Kihou, C. H. Lee, Y. Kotani, K. Ono, S. K. Mo, Z. Hussain, Z.-X. Shen, H. Harima, S. Uchida, and A. Fujimori, Phys. Rev. B **89**, 195138 (2014).
[11] N. Xu, C. E. Matt, P. Richard, A. van Roekeghem, S. Biermann, X. Shi, S.-F. Wu, H. W. Liu, D. Chen, T. Qian, N. C. Plumb, M. Radović, Hangdong Wang, Qianhui Mao, Jianhua Du, Minghu Fang, J. Mesot, H. Ding, and M. Shi, Phys. Rev. B **92**, 081116(R) (2015).
[12] P. Zhang, P. Richard, T. Qian, Y.-M. Xu, X. Dai, and H. Ding, Rev. Sci. Instrum. **82**, 043712 (2011).
[13] N. Xu, P. Richard, A. van Roekeghem, P. Zhang, H. Miao, W.-L. Zhang, T. Qian, M. Ferrero, A. S. Sefat, S. Biermann, and H. Ding, Phys. Rev. X **3**, 011006 (2013).
[14] P. Richard, K. Nakayama, T. Sato, M. Neupane, Y.-M. Xu, J. H. Bowen, G. F. Chen, J. L. Luo, N. L. Wang, X. Dai, Z. Fang, H. Ding, and T. Takahashi, Phys. Rev. Lett. **104**, 137001 (2010).
[15] S. F. Wu, P. Richard, A. van Roekeghem, S. M. Nie, H. Miao, N. Xu, T. Qian, B. Saparov, Z. Fang, S. Biermann, Athena S. Sefat, and H. Ding, Phys. Rev. B **91**, 235109 (2015).
[16] E. Razzoli, C. E. Matt, M. Kobayashi, X.-P. Wang, V. N. Strocov, A. van Roekeghem, S. Biermann, N. C. Plumb, M. Radovic, T. Schmitt, C. Capan, Z. Fisk, P. Richard, H. Ding, P. Aebi, J. Mesot, and M. Shi, Phys. Rev. B **91**, 214502 (2015).
[17] S. Biermann, in *Encyclopedia of Materials: Science and Technology*, edited by K. H. Jürgen Buschow, R. W. Cahn, M. C. Flemings, and B. Ilschner (print) and E. J. Kramer, S. Mahajan, and P. Veyssière (updates) (Elsevier, Oxford, 2006), pp. 1–9.
[18] F. Aryasetiawan, M. Imada, A. Georges, G. Kotliar, S. Biermann, and A. I. Lichtenstein, Phys. Rev. B **70**, 195104 (2004).
[19] L. Vaugier, H. Jiang, and S. Biermann, Phys. Rev. B **86**, 165105 (2012).
[20] Markus Aichhorn, Leonid Pourovskii, Veronica Vildosola, Michel Ferrero, Olivier Parcollet, Takashi Miyake, Antoine Georges, and Silke Biermann, Phys. Rev. B **80**, 085101 (2009).
[21] T. Miyake, L. Pourovskii, V. Vildosola, S. Biermann, and A. Georges, J. Phys. Soc. Jpn. **77**, 99 (2008).
[22] A. van Roekeghem, T. Ayral, J. M. Tomczak, M. Casula, N. Xu, H. Ding, M. Ferrero, O. Parcollet, H. Jiang, and S. Biermann, Phys. Rev. Lett. **113**, 266403 (2014).
[23] V. I. Anisimov, J. Zaanen, and O. K. Andersen, Phys. Rev. B **44**, 943 (1991).
[24] P. Werner, M. Casula, T. Miyake, F. Aryasetiawan, A. J. Millis, and S. Biermann, Nat. Phys. **8**, 331 (2012).
[25] P. Werner, E. Gull, M. Troyer, and A. J. Millis, Phys. Rev. Lett. **101**, 166405 (2008).
[26] K. Haule and G. Kotliar, New J. Phys. **11**, 025021 (2009).
[27] L. de' Medici, J. Mravlje, and A. Georges, Phys. Rev. Lett. **107**, 256401 (2011).
[28] T. Miyake, K. Nakamura, R. Arita, and M. Imada, J. Phys. Soc. Jpn. **79**, 044705 (2010).
[29] R. S. Dhaka, Y. Lee, V. K. Anand, D. C. Johnston, B. N. Harmon, and A. Kaminski, Phys. Rev. B **87**, 214516 (2013).
[30] B. Cheng, B. F. Hu, R. H. Yuan, T. Dong, A. F. Fang, Z. G. Chen, G. Xu, Y. G. Shi, P. Zheng, J. L. Luo, and N. L. Wang, Phys. Rev. B **85**, 144426 (2012).